Electronic Supplementary Information

Enhancing a long-range salt bridge with intermediate aromatic and nonpolar amino acids

Mason S. Smith,[a] Wendy M. Billings,[a] Frank G. Whitby,[b] McKenzie B. Miller,[a] and Joshua L. Price[a*]

[a]Department of Chemistry and Biochemistry, Brigham Young University, Provo, Utah 84602, United States

[b]Department of Biochemistry, University of Utah, Salt Lake City, Utah 84112, United States

1. Protein Synthesis, Purification, and Characterization

Peptides **1**–**24** and their sequence variants (sequences shown in Supplementary Table 1) were synthesized as C-terminal amides, by microwave-assisted solid-phase peptide synthesis, using a standard Fmoc Nα protection strategy as described previously.[1] Fmoc-protected amino acids were activated by 2-(1H-benzotriazole-1-yl)-1,1,3,3-tetramethyluronium hexafluorophosphate (HBTU) and N-hydroxybenzotriazole hydrate (HOBt), all purchased from Advanced ChemTech. NovaSyn TGR resin was purchased from EMD Biosciences. Peptide **1CW** (the S14C mutant of peptide **8**) was synthesized previously.[1]

Peptides were synthesized on a 12.5 μmol scale. A general protocol for manual solid-phase peptide synthesis follows: NovaSyn TGR resin (52.1 mg, 12.5 μmol at 0.24 mmol/g resin loading) was aliquotted into a fritted polypropylene syringe and allowed to swell first in CH_2Cl_2, and then in dimethylformamide (DMF). Solvent was drained from the resin using a vacuum manifold. To remove the Fmoc protecting group on the resin-linked amino acid, 0.625 mL of 20% piperidine in DMF was added to the resin, and the resulting mixture was allowed to sit at room temperature for 1 minute. The deprotection solution was then drained from the resin with a vacuum manifold. An additional 1.25 mL of 20% piperidine in DMF was then added to the resin, and the reaction vessel was placed in the microwave. The temperature was ramped from room temperature to 80°C over the course of 2 minutes and held at 80°C for 2 minutes. The deprotection solution was drained from the resin using a vacuum manifold, and the resin was rinsed five times with DMF. The Fmoc deprotection solution was changed after an aspartate residue was coupled to avoid aspartimide formation. The modified deprotection solution (0.625 mL of 5% m/v piperizine + 0.1 M HOBT in DMF) was added to the resin, the resulting mixture was allowed to sit at room temperature for 1 minute. The deprotection solution was drained from the resin with a vacuum manifold. An additional 0.625 mL of modified deprotection solution was then added to the resin, and the reaction vessel was placed in the microwave. The temperature was ramped from room temperature to 75°C over the course of 2 minutes and held at 75°C for 3 minutes.

For coupling of an activated amino acid, we prepared a stock coupling solution of 100 mL NMP, 3.17 g HBTU (0.01 mol, 0.1 M) and 1.53 g HOBt (0.01 mol, 0.1 M) for a final concentration of 0.1 M HBTU and 0.1 M HOBt. The desired Fmoc-protected amino acid (125 μmol, 5 eq) was dissolved by vortexing in 1.25 mL coupling solution (125 μmol, 5 eq HBTU; 125 μmol, 5 eq HOBt). To the dissolved amino acid solution was added 44 μL DIEA (250 μmol, 10 eq). The resulting mixture was vortexed briefly and allowed to react for at least 1 min. The activated amino acid solution was then added to the resin, and the reaction vessel was placed in the microwave. The temperature was ramped from room temperature to 70°C over 2 minutes and held at 70°C for 4 minutes. Following the coupling reaction, the activated amino acid solution was drained from the resin with a

vacuum manifold, and the resin was subsequently rinsed five times with DMF. The cycles of deprotection and coupling were alternately repeated to give the desired full-length protein.

Acid-labile side-chain protecting groups were globally removed and proteins were cleaved from the resin by stirring the resin for ~4h in a solution of phenol (0.0625 g), water (62.5 μL), thioanisole (62.5 μL), ethanedithiol (31 μL) and triisopropylsilane (12.5 μL) in trifluoroacetic acid (TFA, 1 mL). Following the cleavage reaction, the TFA solution was drained from the resin, the resin was rinsed with additional TFA. Proteins were precipitated from the TFA solution by addition of diethyl ether (~40 mL). Following centrifugation, the ether was decanted, and the pellet was dissolved in ~40mL 1:1 H_2O/MeCN, frozen and lyophilized to remove volatile impurities. The resulting powder was stored at -20°C until purification.

Immediately prior to purification, the crude protein was dissolved in 1:1 H_2O/MeCN. Proteins were purified by preparative reverse-phase high performance liquid chromatography (HPLC) on a C18 column using a linear gradient of water in acetonitrile with 0.1% v/v TFA. Fractions containing the desired protein product were pooled, frozen, and lyophilized. Proteins were identified by electrospray ionization time of flight mass spectrometry (ESI-TOF); expected and observed exact masses mass spectra appear in Table 1. Protein purity was assessed by Analytical HPLC.

Supplementary Table 1. Sequences and expected and observed exact masses for peptides **1-24** and their derivatives.

Peptide	Sequence	z	Expected $[M+z\cdot H^+]/z$	Observed $[M+z\cdot H^+]/z$
1	Ac-EVEALEKKVEALEWKVQKLEKKVEALEHGWDGR-$CONH_2$	4	987.04	987.06
2	Ac-EVEALEKKVAALEWKVQKLEKKVEALEHGWDGR-$CONH_2$	4	972.54	972.56
3	Ac-EVEALEKKVEALEWKVQALEKKVEALEHGWDGR-$CONH_2$	4	972.77	972.81
4	Ac-EVEALEKKVAALEWKVQALEKKVEALEHGWDGR-$CONH_2$	4	958.27	958.31
5	Ac-EVEALEKKVEALESKVQKLEKKVEALEHGWDGR-$CONH_2$	4	962.28	962.28
6	Ac-EVEALEKKVAALESKVQKLEKKVEALEHGWDGR-$CONH_2$	4	947.77	947.76
7	Ac-EVEALEKKVEALESKVQALEKKVEALEHGWDGR-$CONH_2$	4	948.01	948.00
8	Ac-EVEALEKKVAALESKVQALEKKVEALEHGWDGR-$CONH_2$	4	933.51	933.52
9	Ac-EVEALEKKVDALEWKVQKLEKKVEALEHGWDGR-$CONH_2$	4	983.53	983.52
9-DWA	Ac-EVEALEKKVDALEWKVQALEKKVEALEHGWDGR-$CONH_2$	4	969.27	969.26
9-DSK	Ac-EVEALEKKVDALESKVQKLEKKVEALEHGWDGR-$CONH_2$	4	958.77	958.76
9-DSA	Ac-EVEALEKKVDALESKVQALEKKVEALEHGWDGR-$CONH_2$	4	944.51	944.50
10	Ac-EVEALEKKVEALEWKVQOLEKKVEALEHGWDGR-$CONH_2$	4	983.53	983.54
10-AWO	Ac-EVEALEKKVAALEWKVQOLEKKVEALEHGWDGR-$CONH_2$	4	969.03	969.05
10-ESO	Ac-EVEALEKKVEALESKVQOLEKKVEALEHGWDGR-$CONH_2$	4	958.77	958.78
10-ASO	Ac-EVEALEKKVAALESKVQOLEKKVEALEHGWDGR-$CONH_2$	4	944.27	944.29
11	Ac-EVEALEKKVAELEWKVQKLEKKVEALEHGWDGR-$CONH_2$	4	987.04	987.03
11-EWA	Ac-EVEALEKKVAELEWKVQALEKKVEALEHGWDGR-$CONH_2$	4	972.77	972.76
11-ESK	Ac-EVEALEKKVAELESKVQKLEKKVEALEHGWDGR-$CONH_2$	4	962.28	962.27
11-ESA	Ac-EVEALEKKVAELESKVQALEKKVEALEHGWDGR-$CONH_2$	5	758.61	758.61
12	Ac-EVEALEKKVKALEWKVQELEKKVEALEHGWDGR-$CONH_2$	4	987.04	987.04
12-KWA	Ac-EVEALEKKVKALEWKVQALEKKVEALEHGWDGR-$CONH_2$	4	972.54	972.54
12-AWE	Ac-EVEALEKKVAALEWKVQELEKKVEALEHGWDGR-$CONH_2$	4	972.77	972.78
12-KSE	Ac-EVEALEKKVKALESKVQELEKKVEALEHGWDGR-$CONH_2$	4	962.28	962.28
12-KSA	Ac-EVEALEKKVKALESKVQALEKKVEALEHGWDGR-$CONH_2$	4	947.77	947.77
12-ASE	Ac-EVEALEKKVAALESKVQELEKKVEALEHGWDGR-$CONH_2$	4	948.01	948.01
13	Ac-EVEALEKKVEALEBKVQKLEKKVEALEHGWDGR-$CONH_2$	4	990.54	990.53
13-ABK	Ac-EVEALEKKVAALEBKVQKLEKKVEALEHGWDGR-$CONH_2$	4	976.04	976.04
13-EBA	Ac-EVEALEKKVEALEBKVQALEKKVEALEHGWDGR-$CONH_2$	4	976.28	976.27
13-ABA	Ac-EVEALEKKVAALEBKVQALEKKVEALEHGWDGR-$CONH_2$	4	961.78	961.77
14	Ac-EVEALEKKVEALEYKVQKLEKKVEALEHGWDGR-$CONH_2$	4	981.28	981.31
14-AYK	Ac-EVEALEKKVAALEYKVQKLEKKVEALEHGWDGR-$CONH_2$	4	966.78	966.80
14-EYA	Ac-EVEALEKKVEALEYKVQALEKKVEALEHGWDGR-$CONH_2$	4	967.02	967.04
14-AYA	Ac-EVEALEKKVAALEYKVQALEKKVEALEHGWDGR-$CONH_2$	4	952.52	952.52
15	Ac-EVEALEKKVEALEJKVQKLEKKVEALEHGWDGR-$CONH_2$	4	984.79	984.88
15-AJK	Ac-EVEALEKKVAALEJKVQKLEKKVEALEHGWDGR-$CONH_2$	4	970.29	970.39
15-EJA	Ac-EVEALEKKVEALEJKVQALEKKVEALEHGWDGR-$CONH_2$	4	970.52	970.62
15-AJA	Ac-EVEALEKKVAALEJKVQALEKKVEALEHGWDGR-$CONH_2$	4	956.02	956.12
16	Ac-EVEALEKKVEALEFKVQKLEKKVEALEHGWDGR-$CONH_2$	4	977.28	977.28
16-AFK	Ac-EVEALEKKVAALEFKVQKLEKKVEALEHGWDGR-$CONH_2$	4	962.78	962.78
16-EFA	Ac-EVEALEKKVEALEFKVQALEKKVEALEHGWDGR-$CONH_2$	4	963.02	963.01
16-AFA	Ac-EVEALEKKVAALEFKVQALEKKVEALEHGWDGR-$CONH_2$	4	948.52	948.51
17	Ac-EVEALEKKVEALEZKVQKLEKKVEALEHGWDGR-$CONH_2$	4	999.77	999.79
17-AZK	Ac-EVEALEKKVAALEZKVQKLEKKVEALEHGWDGR-$CONH_2$	4	985.27	985.27
17-EZA	Ac-EVEALEKKVEALEZKVQALEKKVEALEHGWDGR-$CONH_2$	4	985.51	985.53
17-AZA	Ac-EVEALEKKVAALEZKVQALEKKVEALEHGWDGR-$CONH_2$	4	971.01	971.03
18	Ac-EVEALEKKVEALEXKVQKLEKKVEALEHGWDGR-$CONH_2$	4	978.80	978.79
18-AXK	Ac-EVEALEKKVAALEXKVQKLEKKVEALEHGWDGR-$CONH_2$	4	964.29	964.29
18-EXA	Ac-EVEALEKKVEALEXKVQALEKKVEALEHGWDGR-$CONH_2$	4	964.53	964.53
18-AXA	Ac-EVEALEKKVAALEXKVQALEKKVEALEHGWDGR-$CONH_2$	4	950.03	950.02
19	Ac-EVEALEKKVEALELKVQKLEKKVEALEHGWDGR-$CONH_2$	4	968.79	968.79
19-ALK	Ac-EVEALEKKVAALELKVQKLEKKVEALEHGWDGR-$CONH_2$	4	954.29	954.29
19-ELA	Ac-EVEALEKKVEALELKVQALEKKVEALEHGWDGR-$CONH_2$	4	954.52	954.52
19-ALA	Ac-EVEALEKKVAALELKVQALEKKVEALEHGWDGR-$CONH_2$	4	940.02	940.02
20	Ac-RMKQLEDRVEALEFKNYKLENEVARLKKLVGER-$CONH_2$	4	1019.07	1019.06
20-AFK	Ac-RMKQLEDRVAALEFKNYKLENEVARLKKLVGER-$CONH_2$	4	1004.57	1004.55
20-EFA	Ac-RMKQLEDRVEALEFKNYALENEVARLKKLVGER-$CONH_2$	4	1004.80	1004.80
20-AFA	Ac-RMKQLEDRVAALEFKNYALENEVARLKKLVGER-$CONH_2$	4	990.30	990.28
20-ESK	Ac-RMKQLEDRVEALESKNYKLENEVARLKKLVGER-$CONH_2$	4	1004.06	1004.08
20-ASK	Ac-RMKQLEDRVAALESKNYKLENEVARLKKLVGER-$CONH_2$	4	989.56	989.54
20-ESA	Ac-RMKQLEDRVEALESKNYALENEVARLKKLVGER-$CONH_2$	4	989.79	989.80
20-ASA	Ac-RMKQLEDRVAALESKNYALENEVARLKKLVGER-$CONH_2$	4	975.29	975.28
21	Ac-RMKQLEDRVAELEFKNYKLENEVARLKKLVGER-$CONH_2$	5	815.46	815.47
21-EFA	Ac-RMKQLEDRVAELEFKNYALENEVARLKKLVGER-$CONH_2$	4	1004.80	1004.88
21-ESK	Ac-RMKQLEDRVAELESKNYKLENEVARLKKLVGER-$CONH_2$	4	1004.06	1004.05
21-ESA	Ac-RMKQLEDRVAELESKNYALENEVARLKKLVGER-$CONH_2$	4	989.79	989.86
22	Ac-RMKQLEDRVAELEXKNYKLENEVARLKKLVGER-$CONH_2$	4	1020.58	1020.58
22-AXK	Ac-RMKQLEDRVAALEXKNYKLENEVARLKKLVGER-$CONH_2$	4	1006.08	1006.07
22-EXA	Ac-RMKQLEDRVAELEXKNYALENEVARLKKLVGER-$CONH_2$	4	1006.31	1006.30
22-AXA	Ac-RMKQLEDRVAALEXKNYALENEVARLKKLVGER-$CONH_2$	4	991.81	991.81
23	Ac-EVEALEKKVEALEFKVQRLEKKVEALEHGWDGR-$CONH_2$	4	984.29	984.27
23-AFR	Ac-EVEALEKKVAALEFKVQRLEKKVEALEHGWDGR-$CONH_2$	4	969.78	969.77
23-ESR	Ac-EVEALEKKVEALESKVQRLEKKVEALEHGWDGR-$CONH_2$	4	969.28	969.27
23-ASR	Ac-EVEALEKKVAALESKVQRLEKKVEALEHGWDGR-$CONH_2$	4	954.77	954.76
24	Ac-EVEALEKKVEALEAKVQKLEKKVEALEHGWDGR-$CONH_2$	4	958.28	958.27
24-AAK	Ac-EVEALEKKVAALEAKVQKLEKKVEALEHGWDGR-$CONH_2$	4	943.78	943.78
24-EAA	Ac-EVEALEKKVEALEAKVQALEKKVEALEHGWDGR-$CONH_2$	4	944.01	944.01
24-AAA	Ac-EVEALEKKVAALEAKVQALEKKVEALEHGWDGR-$CONH_2$	3	1239.01	1239.01

2. Biophysical Characterization of Peptides 1–24

2.1. Self-association Properties of Peptides 1–24: Size Exclusion Chromatography

Previously characterized peptide **1CW** adopts a homotrimeric self-association state in solution, whereas GCN4 adopts a homodimeric self-association state in solution. The large number of peptides explored here (78 peptides including **1**–**24** and their sequence variants shown in Supplementary Table 1) precluded the use of time- and resource-intensive sedimentation equilibrium experiments to characterize their self-association properties. Consequently, we used the higher throughput size exclusion chromatography to characterize the self-association properties of **1**–**24** (and their sequence variants) by comparing their retention times on a size-exclusion column to the retention times of homotrimeric **1CW**, homodimeric **GCN4** and monomeric α-helical **PSBD36**.[1-3]

Size exclusion chromatography (SEC) was done on a Shimadzu HPLC instrument using a Phenomenex yarra 3u sec-3000 column (batches 1 and 2) or a Zenix-C SEC 100 column (batches 3 and 4). The columns were calibrated with internal **1CW**, **GCN4,** and **PSBD36** standards. Previous characterization of **1CW, GCN4,** and **PSBD36** by sedimentation equilibrium analytical ultracentrifugation under analogous buffer conditions demonstrates that **1CW** adopts a trimeric association state; that **GCN4** adopts a dimeric state; and that **PSBD36** is an α-helical monomer.

The retention times derived from SEC experiments on peptides **1-19** and **23-26** are very close to that of trimeric **1CW**, suggesting that these variants likewise adopt a trimeric association state. Similarly, the retention times derived from SEC experiments on peptides **20-22** are close to that of dimeric **GCN4**, suggesting that these variants likewise adopt a dimeric association state. Moreover, published peptide **coil-V_aL_d** (which has the same sequence as peptide **5**, except that **5** has four additional C-terminal residues) crystallizes as a trimer,[4] as do other coiled-coil peptides in which beta-branched non-polar residues (i.e. Ile and/or Val) occupy *a*-positions and Leu occupies *d*-positions in the canonical heptad repeat.[5] Therefore, we are reasonably confident that **1-19** and **23-24** adopt trimeric association states and that **20-22** adopt dimeric association states state.

Supplementary Table 2. Retention times of helical peptides on a Phenomenex Yarra 3u sec-3000 column.

Batch 1			
Peptide	**Calculated MW (Da)**	**Retention Time (min)**	**Inferred association state**
1CW (trimer standard)	11017	10.50	
8	11016	10.50	trimer
16	11541	10.54	trimer
16-EFA	11367	10.38	trimer
16-AFK	11370	10.51	trimer
5	11361	10.43	trimer
6	11190	10.51	trimer
7	11187	10.35	trimer
16-AFA	11196	10.47	trimer
14-AYA	11244	10.45	trimer
14-EYA	11416	10.35	trimer
14-AYK	11419	10.50	trimer
14-EYA	11590	10.43	trimer
4	11313	10.50	trimer
3	11484	10.37	trimer
2	11488	10.60	trimer
1	11659	10.55	trimer
18-AXA	11214	10.44	trimer
18-EXA	11385	10.33	trimer
18-AXK	11389	10.52	trimer
18	11560	10.41	trimer
23-AFR	11452	10.56	trimer
23	11623	10.43	trimer
23-ASR	11271	10.52	trimer
23-ESR	11442	10.41	trimer
11-EWA	11367	10.43	trimer
11	11541	10.56	trimer
11-ESA	11187	10.41	trimer
11-ESK	11361	10.52	trimer
12-KSA	11190	10.60	trimer
12-ASE	11187	10.38	trimer
12-KSE	11361	10.47	trimer
12-KWA	11488	10.76	trimer
12-AWE	11484	10.44	trimer
12	11659	10.51	trimer
Batch 2			
Peptide	**Calculated MW (Da)**	**Retention Time (min)**	**Inferred association state**
1CW (trimer standard)	11017	10.19	
9-DSA	11325	10.08	trimer
9-DSK	11496	10.26	trimer
9-DWA	11622	10.21	trimer
9	11793	10.34	trimer
10-ASO	11322	10.33	trimer
10-AWO	11619	10.49	trimer
10-ESO	11496	10.21	trimer
10	11793	10.29	trimer
17-AZA	11652	10.20	trimer
17-AZK	11823	10.28	trimer
17-EZA	11826	10.08	trimer
17	11997	10.22	trimer

Supplementary Table 3. Retention times of helical peptides on a Zenix-C SEC 100 column.

Batch 3			
Peptide	**Calculated MW (Da)**	**Retention Time (min)**	**Inferred association state**
1CW (trimer standard)	11199	8.83	
GCN4 (dimer standard)	8131	9.43	
PSBD36 (monomer standard)	4001	10.51	
15-AJA	11422	8.97	trimer
15-EJA	11593	8.83	trimer
15-AJK	11596	8.99	trimer
15-EJK	11767	8.88	trimer
13-ABA	11491	9.05	trimer
13-EBA	11662	8.95	trimer
13-ABK	11665	9.10	trimer
13-EBK	11836	8.95	trimer
24-AAA	11104	8.86	trimer
24-EAA	11275	8.73	trimer
24-AAK	11278	8.86	trimer
24	11449	8.83	trimer
20-ESA	7909	9.13	dimer
20-ASA	7794	9.52	dimer
20-ASK	7911	9.50	dimer
20-AFA	7915	10.30	dimer/monomer
20-AFK	8031	10.23	dimer/monomer
20-ESK	8025	9.15	dimer
20-EFA	8029	9.39	dimer
20	8145	9.46	dimer
21-ESA	7909	9.44	dimer
21-ESK	8025	9.39	dimer
21-EFA	8029	9.81	dimer
21-EFK	8145	9.73	dimer
22-AXA	7927	10.34	dimer/monomer
22-EXA	8041	9.83	dimer
22-AXK	8043	10.33	dimer/monomer
22	8157	9.79	dimer
Batch 4			
Peptide	**Calculated MW (Da)**	**Retention Time (min)**	**Inferred association state**
1CW (trimer standard)	11199	9.01	
25	11275	8.93	trimer
26	11449	9.09	trimer
1CW (trimer standard)	11199	9.04	trimer
19	11575	8.94	trimer
19-ALK	11404	8.96	trimer
19-ELA	11401	9.07	trimer
1CW (trimer standard)	11199	9.11	trimer
19-ALA	11229	9.23	trimer

2.2. Secondary Structure and Folding Free Energy of Peptides 1–24: Circular Dichroism Spectropolarimetry

Measurements were made with an Aviv 420 Circular Dichroism Spectropolarimeter, using quartz cuvettes with a path length of 0.1 cm. Protein solutions were prepared in 20 mM sodium phosphate buffer, pH 7, and protein concentrations were determined spectroscopically based on tyrosine and tryptophan absorbance at 280 nm in 6 M guanidine hydrochloride + 20 mM sodium phosphate (ε_{Trp} = 5690 $M^{-1}cm^{-1}$, ε_{Tyr} = 1280 $M^{-1}cm^{-1}$).[6] CD spectra of 30 μM solutions were obtained from 260 to 200 nm at 25°C. Variable temperature CD data were obtained at least in triplicate by monitoring the molar ellipticity at 222 nm of 30 μM solutions each protein variant (30 μM) in 20 mM sodium phosphate (pH 7) from 1 to 95°C at 2 °C intervals, with 120 s equilibration time between data points and 30 s averaging time.

Triplicate variable temperature CD data for **1-19, 23-26** and their individual variants were fit globally to a two-state model for thermally-induced unfolding of helix-bundle trimers as shown in equations S1—S9 (see below for sedimentation equilibrium evidence that these 1CW variants are, in fact, trimers).

In this two state model, 3 peptide monomers **M** are in equilibrium with the helix-bundle trimer **T**, where the position of equilibrium is determined by folding equilibrium constant **K**:

$$3M \underset{}{\overset{K}{\rightleftharpoons}} T \tag{S1}$$

In turn, **K** is defined by the equation S2:

$$K = \frac{[T]}{[M]^3} \tag{S2}$$

where [**T**] and [**M**] are the concentrations of helix-bundle trimer and peptide monomer, respectively. The total concentration of peptide in solution **P** is defined by the equation S3:

$$P = [M] + 3[T] \tag{S3}$$

By combining equations S2 and S3, we can obtain an expression for **P** that depends only on [**M**] and on $\mathbf{K_f}$, as shown in equation S4:

$$P = [M] + 3K[M]^3 \tag{S4}$$

In equation S4, **P** is a constant, **K** is a temperature-dependent function (that is constant at a given temperature), and [**M**] is unknown. Rearranging equation S4 results in the following polynomial equation that is cubic in [**M**]:

$$0 = [M]^3 + \frac{[M]}{3K} - \frac{P}{3K} \tag{S5}$$

Using MATLAB, we found the three roots of this polynomial, two of which are complex, whereas the third is real. The real root of equation (S5) provides an expression for [**M**] that depends only on **P** and $\mathbf{K_f}$, as shown in equation (S6):

$$[M] = \left(\frac{P}{6K} + \left(\frac{1}{729K^3} + \frac{P^2}{36K^2}\right)^{\frac{1}{2}}\right)^{\frac{1}{3}} - \frac{1}{9K\left(\frac{P}{6K} + \left(\frac{1}{729K^3} + \frac{P^2}{36K^2}\right)^{\frac{1}{2}}\right)^{\frac{1}{3}}} \tag{S6}$$

As described above, **K** is a temperature-dependent function that is constant at a given temperature. **K** is related to the temperature-dependent folding free energy $\mathbf{\Delta G_f}$ according to equation S7:

$$K = exp\left(\frac{-\Delta G_f}{RT}\right) \tag{S7}$$

where R is the universal gas constant (0.0019872 kcal/mol/K). In turn, the temperature dependence of $\mathbf{\Delta G_f}$ can be defined by the following first order polynomial:

$$\Delta G_f = \Delta G_o + \Delta G_1(T - T_o) \tag{S8}$$

where T is temperature in Kelvin; $\mathbf{\Delta G_0}$ and $\mathbf{\Delta G_1}$ are parameters to be determined via least-squares regression; and T_0 is an arbitrary reference temperature, ideally chosen to be near the midpoint of the unfolding transition. By combining equations S6–S8, we now have an expression for [**M**] as a function of temperature that depends only on $\mathbf{\Delta G_0}$, $\mathbf{\Delta G_1}$, **P** and reference temperature $\mathbf{T_0}$.

We can use this expression for [**M**] to fit the variable temperature CD data [θ] to equation S9, using the actual protein concentration in solution for **P**; using a fixed arbitrary value for T_0 (343.15 K); and then varying $\mathbf{\Delta G_0}$ and $\mathbf{\Delta G_1}$ as parameters of the fit so as to minimize the sum of the squared residuals.

$$[\theta] = (u_o)\left(1 - \frac{3K[M]^3}{P}\right) + (f_o + f_1 T)\left(\frac{3K[M]^3}{P}\right) \quad \text{(S9)}$$

In equation S9, T is the temperature in Kelvin; u_o defines a horizontal post-transition baseline; and f_o and f_1 are the intercept and slope of the pre-transition baseline, respectively. We fit the variable trimer variable temperature CD data using distinct ΔG_0 and ΔG_1 values for each peptide; distinct u_o and f_o values for each replicate data set of each peptide and a global value for f_1 across all replicate data sets and peptides.

Triplicate variable temperature CD data for each **20-22** and their individual variants were fit globally to a two-state model for thermally-induced unfolding of helix-bundle dimers as shown in equations S1—S9 (see below for sedimentation equilibrium evidence that these GCN4-p1 variants are dimers).

In this two state model, 2 peptide monomers **M** are in equilibrium with the helix-bundle dimer **D**, where the position of equilibrium is determined by folding equilibrium constant **K**:

$$2M \overset{K}{\rightleftharpoons} D \quad \text{(S10)}$$

In turn, **K** is defined by the equation S11:

$$K = \frac{[D]}{[M]^2} \quad \text{(S11)}$$

where [**T**] and [**M**] are the concentrations of helix-bundle trimer and peptide monomer, respectively. The total concentration of peptide in solution **P** is defined by the equation S3:

$$P = [M] + 2[D] \quad \text{(S12)}$$

By combining equations S12 and S11, we can obtain an expression for **P** that depends only on [**M**] and on $\mathbf{K_f}$, as shown in equation S4:

$$P = [M] + 2K[M]^2 \quad \text{(S13)}$$

In equation S13, **P** is a constant, **K** is a temperature-dependent function (that is constant at a given temperature), and [**M**] is unknown. Rearranging equation S13 results in the following quadratic:

$$0 = [M]^2 + [M] - P \quad \text{(S14)}$$

The solution the the quadratic (S14) provides an expression for [**M**] that depends only on **P** and **K**, as shown in equation (S15):

$$[M] = \frac{\sqrt{1 + 8KP} + 1}{4K} \tag{S15}$$

described above, **K** is a temperature-dependent function that is constant at a given temperature. In turn, the temperature dependence of $\mathbf{\Delta G_f}$ for the dimer can be defined by the following second order polynomial:

$$\Delta G_f = \Delta G_o + \Delta G_1(T - T_o) + \Delta G_2(T - T_o)^2 \tag{S16}$$

T is temperature in Kelvin; $\mathbf{\Delta G_0}$, $\mathbf{\Delta G_1}$ and $\mathbf{\Delta G_2}$ are parameters to be determined via least-squares regression; and T_0 is an arbitrary reference temperature, also chosen near the midpoint of the unfolding transition. By combining equations, we now have an expression for [**M**] as a function of temperature that depends only on $\mathbf{\Delta G_0}$, $\mathbf{\Delta G_1}$, **P** and reference temperature $\mathbf{T_0}$.

We can use this expression for [**M**] to fit the variable temperature CD data [θ] to equation S9, using the actual protein concentration in solution for **P**; using a fixed arbitrary value for T_0 (343.15 K); and then varying $\mathbf{\Delta G_0}$ and $\mathbf{\Delta G_1}$ as parameters of the fit so as to minimize the sum of the squared residuals.

$$[\theta] = (u_o)(1 - Ffit) + (f_o + f_1 T)(Ffit) \tag{S17}$$

In equation S18, T is the temperature in Kelvin; u_o defines a horizontal post-transition baseline; and f_o and f_1 are the intercept and slope of the pre-transition baseline, respectively. Ffit is the fraction folded as defined by equation (S19) of the protein at temperature T.

$$Ffit = 1 + \left(\frac{1}{4KP}\right) - \left(\frac{1}{2KP} + \frac{1}{16K^2P^2}\right)^{\frac{1}{2}} \tag{S18}$$

We fit the dimer variable temperature CD data using distinct $\mathbf{\Delta G_0}$, $\mathbf{\Delta G_1}$ and $\mathbf{\Delta G_2}$ values for each peptide; distinct u_o and f_o values for each replicate data set of each peptide and a global value for f_1 across all replicate data sets and peptides.

Folding free energies and molar ellipticity data for homotrimeric peptides **1**-**19**, **23**, and **24** (and their sequence derivatives) are shown in Supplementary Tables 4 and 5 and plotted in Supplementary Figures 1 and 2; data for GCN4-based homodimeric peptides **20**–**22** (and their sequence derivatives) are shown in Supplementary Table 6 and plotted in Supplementary Figure 3. Far-UV CD spectra and variable temperature CD data for these variants are consistent with α-helical coiled-coil quaternary structure. An example is shown below for peptide **1** in Supplementary Figure 4. The magnitude of molar ellipticity at 222 nm and 208 nm ($[\theta]_{222}$ and $[\theta]_{208}$, the characteristic minima in the CD spectra of α-helical proteins) varies widely from compound to compound. This variation is not well-correlated with folding free energy for the homotrimeric coiled-coil peptides **1**-**19** and **23**, suggesting that the absolute values of $[\theta]_{222}$ and $[\theta]_{208}$ are not well-correlated with the stability of the cooperatively-folded coiled-coil quaternary structure. In contrast, variation in $[\theta]_{222}$ and $[\theta]_{208}$ are reasonably well-correlated with folding free energy for homodimeric coiled-coil peptides **20**–**22**. In any case, the ratio between $[\theta]_{222}/[\theta]_{208}$ does not vary substantial from ~1.1 (a value which has been described previously as diagnostic for coiled coils), suggesting that the variations in the absolute values of $[\theta]_{222}$ and $[\theta]_{208}$ among homotrimeric **1**-**19** and **23** or among homodimeric **20**–**22** are not associated with dramatic differences in coiled-coil quaternary structure.

Supplementary Table 4. Folding free energies for **1-8**, **14-19** and **23** and their derivatives at 343.15 K in 20 mM sodium phosphate (pH 7).*

Peptide	Sequence	ΔG_f (kcal/mol)	$[\theta]_{222}$ (deg cm^2 dmol^{-1}) x 10^{-3}	$[\theta]_{208}$ (deg cm^2 dmol^{-1}) x 10^{-3}	$[\theta]_{222}/[\theta]_{208}$
1	Ac-EVEALEKKV**E**ALE**W**KVQ**K**LEKKVEALEHGWDGR-$CONH_2$	-17.23 ± 0.03	-37.6	-33.7	1.12
2	Ac-EVEALEKKV**AA**LE**W**KVQ**K**LEKKVEALEHGWDGR-$CONH_2$	-16.84 ± 0.03	-27.3	-24.6	1.11
3	Ac-EVEALEKKV**E**ALE**W**KVQ**A**LEKKVEALEHGWDGR-$CONH_2$	-15.24 ± 0.03	-19.3	-17.0	1.14
4	Ac-EVEALEKKV**AA**LE**W**KVQ**A**LEKKVEALEHGWDGR-$CONH_2$	-17.03 ± 0.04	-21.1	-20.1	1.05
5	Ac-EVEALEKKV**E**ALE**S**KVQ**K**LEKKVEALEHGWDGR-$CONH_2$	-14.09 ± 0.02	-23.7	-23.1	1.03
6	Ac-EVEALEKKV**AA**LE**S**KVQ**K**LEKKVEALEHGWDGR-$CONH_2$	-15.87 ± 0.03	-26.7	-24.5	1.09
7	Ac-EVEALEKKV**E**ALE**S**KVQ**A**LEKKVEALEHGWDGR-$CONH_2$	-15.48 ± 0.02	-35.5	-33.7	1.06
8	Ac-EVEALEKKV**AA**LE**S**KVQ**A**LEKKVEALEHGWDGR-$CONH_2$	-16.39 ± 0.04	-19.4	-18.2	1.07
14	Ac-EVEALEKKV**E**ALE**Y**KVQ**K**LEKKVEALEHGWDGR-$CONH_2$	-14.96 ± 0.02	-20.9	-20.0	1.04
14-AYK	Ac-EVEALEKKV**AA**LE**Y**KVQ**K**LEKKVEALEHGWDGR-$CONH_2$	-14.34 ± 0.03	-10.4	-10.0	1.04
14-EYA	Ac-EVEALEKKV**E**ALE**Y**KVQ**A**LEKKVEALEHGWDGR-$CONH_2$	-15.51 ± 0.03	-23.0	-21.8	1.06
14-AYA	Ac-EVEALEKKV**AA**LE**Y**KVQ**A**LEKKVEALEHGWDGR-$CONH_2$	-16.82 ± 0.06	-18.4	-17.2	1.07
15	Ac-EVEALEKKV**E**ALE**J**KVQ**K**LEKKVEALEHGWDGR-$CONH_2$	-14.58 ± 0.02	-24.3	-22.8	1.07
15-AJK	Ac-EVEALEKKV**AA**LE**J**KVQ**K**LEKKVEALEHGWDGR-$CONH_2$	-16.10 ± 0.04	-25.5	-24.4	1.05
15-EJA	Ac-EVEALEKKV**E**ALE**J**KVQ**A**LEKKVEALEHGWDGR-$CONH_2$	-15.71 ± 0.03	-32.0	-30.0	1.07
15-AJA	Ac-EVEALEKKV**AA**LE**J**KVQ**A**LEKKVEALEHGWDGR-$CONH_2$	-17.24 ± 0.04	-25.9	-24.3	1.07
16	Ac-EVEALEKKV**E**ALE**F**KVQ**K**LEKKVEALEHGWDGR-$CONH_2$	-14.66 ± 0.02	-21.5	-19.8	1.09
16-AFK	Ac-EVEALEKKV**AA**LE**F**KVQ**K**LEKKVEALEHGWDGR-$CONH_2$	-16.18 ± 0.03	-25.3	-22.6	1.12
16-EFA	Ac-EVEALEKKV**E**ALE**F**KVQ**A**LEKKVEALEHGWDGR-$CONH_2$	-15.05 ± 0.03	-21.0	-19.2	1.09
16-AFA	Ac-EVEALEKKV**AA**LE**F**KVQ**A**LEKKVEALEHGWDGR-$CONH_2$	-16.95 ± 0.04	-24.0	-22.4	1.07
17	Ac-EVEALEKKV**E**ALE**Z**KVQ**K**LEKKVEALEHGWDGR-$CONH_2$	-14.11 ± 0.02	-26.3	-24.1	1.09
17-AZK	Ac-EVEALEKKV**AA**LE**Z**KVQ**K**LEKKVEALEHGWDGR-$CONH_2$	-15.92 ± 0.03	-29.2	-26.2	1.12
17-EZA	Ac-EVEALEKKV**E**ALE**Z**KVQ**A**LEKKVEALEHGWDGR-$CONH_2$	-14.61 ± 0.03	-22.2	-18.8	1.18
17-AZA	Ac-EVEALEKKV**AA**LE**Z**KVQ**A**LEKKVEALEHGWDGR-$CONH_2$	-16.63 ± 0.03	-25.1	-21.9	1.14
18	Ac-EVEALEKKV**E**ALE**X**KVQ**K**LEKKVEALEHGWDGR-$CONH_2$	-15.96 ± 0.03	-23.5	-21.9	1.07
18-AXK	Ac-EVEALEKKV**AA**LE**X**KVQ**K**LEKKVEALEHGWDGR-$CONH_2$	-17.17 ± 0.07	-21.4	-19.5	1.09
18-EXA	Ac-EVEALEKKV**E**ALE**X**KVQ**A**LEKKVEALEHGWDGR-$CONH_2$	-16.53 ± 0.06	-18.9	-17.3	1.09
18-AXA	Ac-EVEALEKKV**AA**LE**X**KVQ**A**LEKKVEALEHGWDGR-$CONH_2$	-18.22 ± 0.06	-24.4	-21.7	1.13
19	Ac-EVEALEKKV**E**ALE**L**KVQ**K**LEKKVEALEHGWDGR-$CONH_2$	-15.78 ± 0.03	-25.3	-24.3	1.04
19-ALK	Ac-EVEALEKKV**AA**LE**L**KVQ**K**LEKKVEALEHGWDGR-$CONH_2$	-17.32 ± 0.04	-24.9	-24.0	1.04
19-ELA	Ac-EVEALEKKV**E**ALE**L**KVQ**A**LEKKVEALEHGWDGR-$CONH_2$	-16.74 ± 0.03	-34.7	-32.8	1.06
19-ALA	Ac-EVEALEKKV**AA**LE**L**KVQ**A**LEKKVEALEHGWDGR-$CONH_2$	-18.77 ± 0.06	-35.0	-33.2	1.06
23	Ac-EVEALEKKV**E**ALE**F**KVQ**R**LEKKVEALEHGWDGR-$CONH_2$	-15.65 ± 0.02	-28.2	-25.5	1.10
23-AFR	Ac-EVEALEKKV**AA**LE**F**KVQ**R**LEKKVEALEHGWDGR-$CONH_2$	-16.84 ± 0.03	-27.2	-24.5	1.11
23-ESR	Ac-EVEALEKKV**E**ALE**S**KVQ**R**LEKKVEALEHGWDGR-$CONH_2$	-14.59 ± 0.02	-28.2	-25.5	1.10
23-ASR	Ac-EVEALEKKV**AA**LE**S**KVQ**R**LEKKVEALEHGWDGR-$CONH_2$	-16.30 ± 0.03	-27.2	-24.5	1.11

*Folding free energies are for association of the monomer into a coiled-coil dimer.

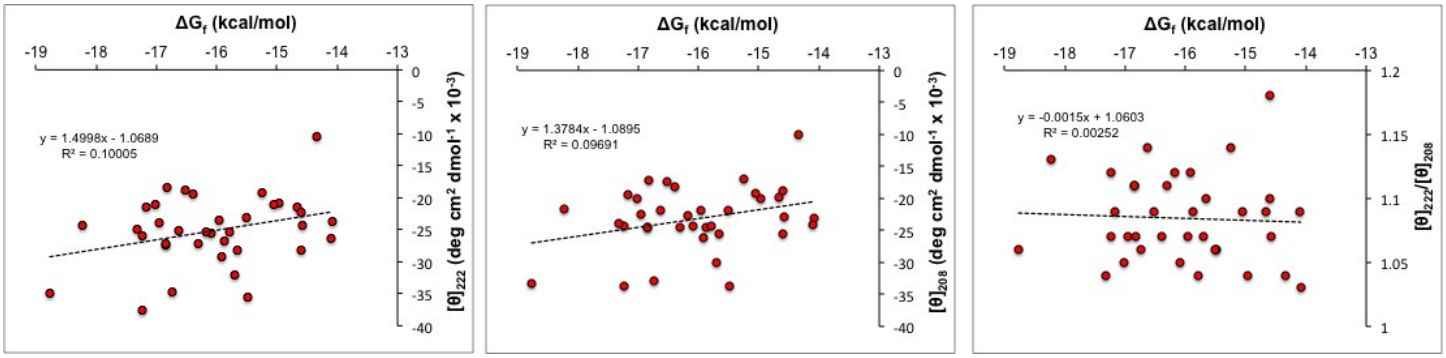

Supplementary Figure 1. Plots of $[\theta]_{222}$, $[\theta]_{208}$, and of $[\theta]_{222}/[\theta]_{208}$ against folding free energy for homotrimeric peptides **1**–**19** and **23** in 20 mM sodium phosphate (pH 7).

Supplementary Table 5. Folding free energies for **1-13**, **24** and their derivatives at 343.15 K in 20 mM sodium phosphate (pH 7) + 1 M Urea.*

Peptide	Sequence	ΔG_f (kcal/mol)	$[\theta]_{222}$ (deg cm^2 dmol^{-1}) x 10^{-3}
1	Ac−EVEALEKKV**E**ALE**W**KVQ**K**LEKKVEALEHGWDGR−CONH$_2$	-16.23 ± 0.05	-44.8
2	Ac−EVEALEKKV**AA**LE**W**KVQ**K**LEKKVEALEHGWDGR−CONH$_2$	-15.73 ± 0.04	-29.5
3	Ac−EVEALEKKV**E**ALE**W**KVQ**A**LEKKVEALEHGWDGR−CONH$_2$	-14.04 ± 0.03	-16.5
4	Ac−EVEALEKKV**AA**LE**W**KVQ**A**LEKKVEALEHGWDGR−CONH$_2$	-15.78 ± 0.05	-20.7
5	Ac−EVEALEKKV**E**ALE**S**KVQ**K**LEKKVEALEHGWDGR−CONH$_2$	-13.42 ± 0.02	-37.9
6	Ac−EVEALEKKV**AA**LE**S**KVQ**K**LEKKVEALEHGWDGR−CONH$_2$	-14.74 ± 0.02	-26.8
7	Ac−EVEALEKKV**E**ALE**S**KVQ**A**LEKKVEALEHGWDGR−CONH$_2$	-14.18 ± 0.02	-36.2
8	Ac−EVEALEKKV**AA**LE**S**KVQ**A**LEKKVEALEHGWDGR−CONH$_2$	-15.30 ± 0.04	-19.2
9	Ac−EVEALEKKV**D**ALE**W**KVQ**K**LEKKVEALEHGWDGR−CONH$_2$	-12.23 ± 0.03	-26.8
9-DWA	Ac−EVEALEKKV**D**ALE**W**KVQ**A**LEKKVEALEHGWDGR−CONH$_2$	-11.53 ± 0.04	-11.8
9-DSK	Ac−EVEALEKKV**D**ALE**S**KVQ**K**LEKKVEALEHGWDGR−CONH$_2$	-10.97 ± 0.04	-15.9
9-DSA	Ac−EVEALEKKV**D**ALE**S**KVQ**A**LEKKVEALEHGWDGR−CONH$_2$	-11.99 ± 0.02	-18.1
10	Ac−EVEALEKKV**E**ALE**W**KVQ**O**LEKKVEALEHGWDGR−CONH$_2$	-13.63 ± 0.01	-25.1
10-AWO	Ac−EVEALEKKV**A**ALE**W**KVQ**O**LEKKVEALEHGWDGR−CONH$_2$	-15.15 ± 0.02	-26.4
10-ESO	Ac−EVEALEKKV**E**ALE**S**KVQ**O**LEKKVEALEHGWDGR−CONH$_2$	-13.05 ± 0.01	-36.1
10-ASO	Ac−EVEALEKKV**A**ALE**S**KVQ**O**LEKKVEALEHGWDGR−CONH$_2$	-13.92 ± 0.01	-22.6
11	Ac−EVEALEKKV**AE**LE**W**KVQ**K**LEKKVEALEHGWDGR−CONH$_2$	-15.94 ± 0.06	-22.2
11-EWA	Ac−EVEALEKKV**AE**LE**W**KVQ**A**LEKKVEALEHGWDGR−CONH$_2$	-16.34 ± 0.07	-21.9
11-ESK	Ac−EVEALEKKV**AE**LE**S**KVQ**K**LEKKVEALEHGWDGR−CONH$_2$	-17.58 ± 0.04	-47.2
11-ESA	Ac−EVEALEKKV**AE**LE**S**KVQ**A**LEKKVEALEHGWDGR−CONH$_2$	-17.27 ± 0.05	-27.3
12	Ac−EVEALEKKV**K**ALE**W**KVQ**E**LEKKVEALEHGWDGR−CONH$_2$	-16.72 ± 0.07	-25.8
12-KWA	Ac−EVEALEKKV**K**ALE**W**KVQ**A**LEKKVEALEHGWDGR−CONH$_2$	-16.46 ± 0.05	-31.3
12-AWE	Ac−EVEALEKKV**AA**LE**W**KVQ**E**LEKKVEALEHGWDGR−CONH$_2$	-17.06 ± 0.06	-38.1
12-KSE	Ac−EVEALEKKV**K**ALE**S**KVQ**E**LEKKVEALEHGWDGR−CONH$_2$	-16.18 ± 0.04	-35.1
12-KSA	Ac−EVEALEKKV**K**ALE**S**KVQ**A**LEKKVEALEHGWDGR−CONH$_2$	-15.30 ± 0.04	-21.6
12-ASE	Ac−EVEALEKKV**AA**LE**S**KVQ**E**LEKKVEALEHGWDGR−CONH$_2$	-16.43 ± 0.07	-37.6
13	Ac−EVEALEKKV**E**ALE**B**KVQ**K**LEKKVEALEHGWDGR−CONH$_2$	-13.31 ± 0.03	-19.6
13-ABK	Ac−EVEALEKKV**AA**LE**B**KVQ**K**LEKKVEALEHGWDGR−CONH$_2$	-14.71 ± 0.05	-17.5
13-EBA	Ac−EVEALEKKV**E**ALE**B**KVQ**A**LEKKVEALEHGWDGR−CONH$_2$	-14.10 ± 0.04	-20.5
13-ABA	Ac−EVEALEKKV**AA**LE**B**KVQ**A**LEKKVEALEHGWDGR−CONH$_2$	-16.30 ± 0.06	-24.4
24	Ac−EVEALEKKV**E**ALE**A**KVQ**K**LEKKVEALEHGWDGR−CONH$_2$	-14.78 ± 0.02	-30.4
24-AAK	Ac−EVEALEKKV**AA**LE**A**KVQ**K**LEKKVEALEHGWDGR−CONH$_2$	-16.66 ± 0.07	-23.5
24-EAA	Ac−EVEALEKKV**E**ALE**A**KVQ**A**LEKKVEALEHGWDGR−CONH$_2$	-16.31 ± 0.06	-29.7
24-AAA	Ac−EVEALEKKV**AA**LE**A**KVQ**A**LEKKVEALEHGWDGR−CONH$_2$	-17.32 ± 0.09	-19.2

*Buffer conditions (i.e., 1 M urea) precluded data collection at 208 nm due to excessively high dynode values. Folding free energies are for association of the monomer into a coiled-coil trimer.

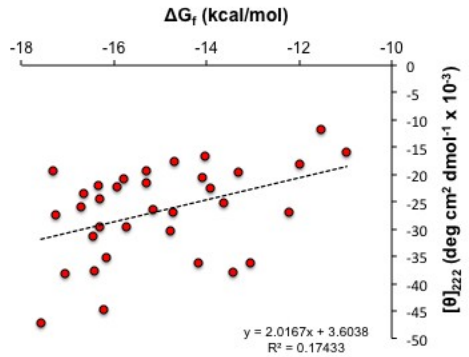

Supplementary Figure 2. Plot of $[\theta]_{222}$ against folding free energy for homotrimeric peptides **1**–**8**, **9**–**13** , and **24** in 20 mM sodium phosphate (pH 7) + 1 M urea.

Supplementary Table 6. Folding free energies for **20-22** and their derivatives at 333.15 K in 20 mM sodium phosphate (pH 7).*

Peptide	Sequence	ΔG_f (kcal/mol)	$[\theta]_{222}$ (deg cm^2 dmol^{-1}) x 10^{-3}	$[\theta]_{208}$ (deg cm^2 dmol^{-1}) x 10^{-3}	$[\theta]_{222}/[\theta]_{208}$
20	Ac−RMKQLEDRV**E**ALE**F**KNY**K**LENEVARLKKLVGER−CONH$_2$	-5.57 ± 0.06	-6.7	-5.9	1.14
20-AFK	Ac−RMKQLEDRV**AA**LE**F**KNY**K**LENEVARLKKLVGER−CONH$_2$	-7.98 ± 0.04	-15.6	-13.4	1.17
20-EFA	Ac−RMKQLEDRV**E**ALE**F**KNY**A**LENEVARLKKLVGER−CONH$_2$	-6.38 ± 0.04	-13.8	-11.8	1.17
20-AFA	Ac−RMKQLEDRV**AA**LE**F**KNY**A**LENEVARLKKLVGER−CONH$_2$	-8.14 ± 0.03	-20.8	-17.8	1.17
20-ESK	Ac−RMKQLEDRV**E**ALE**S**KNY**K**LENEVARLKKLVGER−CONH$_2$	-4.92 ± 0.08	-7.3	-6.6	1.09
20-ASK	Ac−RMKQLEDRV**AA**LE**S**KNY**K**LENEVARLKKLVGER−CONH$_2$	-7.43 ± 0.02	-18.8	-17.5	1.07
20-ESA	Ac−RMKQLEDRV**E**ALE**S**KNY**A**LENEVARLKKLVGER−CONH$_2$	-5.85 ± 0.02	-17.8	-16.5	1.08
20-ASA	Ac−RMKQLEDRV**AA**LE**S**KNY**A**LENEVARLKKLVGER−CONH$_2$	-7.81 ± 0.04	-20.1	-18.3	1.10
21	Ac−RMKQLEDRVA**E**LE**F**KNY**K**LENEVARLKKLVGER−CONH$_2$	-7.97 ± 0.04	-23.8	-21.2	1.12
21-EFA	Ac−RMKQLEDRVA**E**LE**F**KNY**A**LENEVARLKKLVGER−CONH$_2$	-7.74 ± 0.02	-30.2	-27.0	1.12
21-ESK	Ac−RMKQLEDRVA**E**LE**S**KNY**K**LENEVARLKKLVGER−CONH$_2$	-5.60 ± 0.05	-8.5	-7.1	1.19
21-ESA	Ac−RMKQLEDRVA**E**LE**S**KNY**A**LENEVARLKKLVGER−CONH$_2$	-7.14 ± 0.02	-20.9	-18.9	1.10
22	Ac−RMKQLEDRVA**E**LE**X**KNY**K**LENEVARLKKLVGER−CONH$_2$	-7.97 ± 0.03	-23.3	-21.4	1.1
22-AXK	Ac−RMKQLEDRVA**A**LE**X**KNY**K**LENEVARLKKLVGER−CONH$_2$	-8.80 ± 0.02	-30.6	-26.5	1.2
22-EXA	Ac−RMKQLEDRVA**E**LE**X**KNY**A**LENEVARLKKLVGER−CONH$_2$	-8.19 ± 0.03	-29.6	-27.1	1.1
22-AXA	Ac−RMKQLEDRVA**A**LE**X**KNY**A**LENEVARLKKLVGER−CONH$_2$	-9.10 ± 0.04	-31.4	-27.2	1.2

*Folding free energies are for association of the monomer into a coiled-coil dimer.

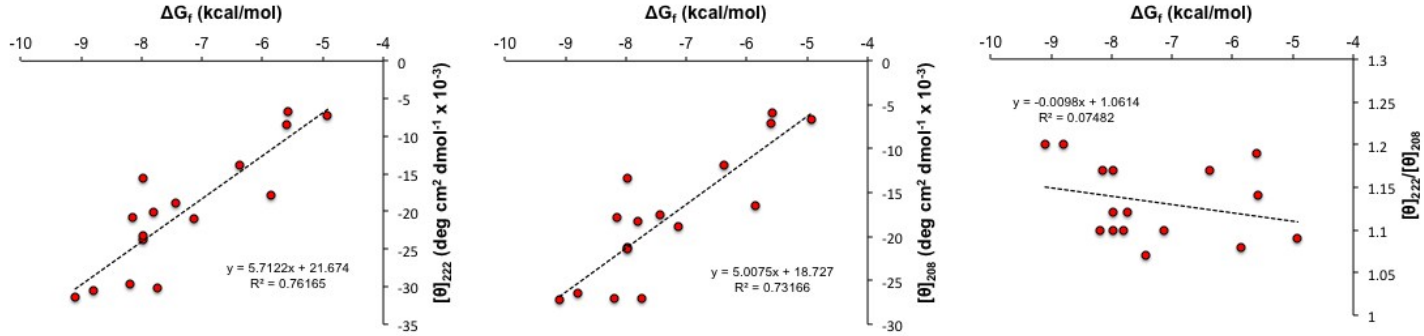

Supplementary Figure 3. Plots of $[\theta]_{222}$, $[\theta]_{208}$, and of $[\theta]_{222}/[\theta]_{208}$ against folding free energy for homodimeric peptides **20**–**22** in 20 mM sodium phosphate (pH 7).

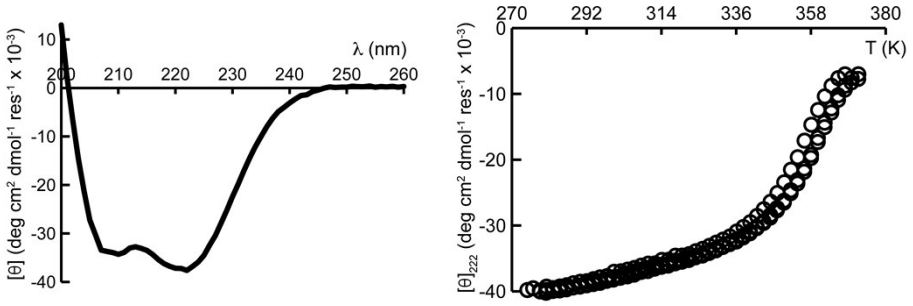

Protein	ΔG_0 (kcal/mol)	ΔG_1 (kcal/mol/K)	T_{ref} (K)	R^2	std error
1	-17.23 ± 0.03	0.195 ± 0.003	343.15	0.9996	0.179

buffer: 20 mM sodium phosphate (pH 7)

Supplementary Figure 4. CD spectrum (line, top left) and triplicate variable temperature CD data (circles, top right) for a 30 μM solution of protein **1** in 20 mM sodium phosphate (pH 7). Parameters used to fit the variable temperature CD data to equations S6–S9 are also shown, with standard errors as indicated.

2.3. Structural similarity of Peptides 1–24: NMR Spectroscopy

We prepared NMR samples for peptides **1**–**24** and their derivatives at 0.2 mM peptide concentration in 20 mM sodium phosphate (pH 7) with 10% D_2O. Samples were transferred to a Varian 500 MHz magnet and we collected 1D ^{1}H NMR spectra of each compound using vnmrJ software. Water suppression was achieved using an Watergate 3-9-19 sequence. We ran 1024 scans with a 2 second relaxation delay and a receiver gain of 30dB. The similarity of the amide regions from the 1D ^{1}H NMR spectra of peptides **1**–**24** and their derivatives suggests that the sequence differences among peptides **1**–**24** and their derivatives do not substantially perturb their global conformational properites relative to each other. Supplementary Figure. 5 shows the overlaid amide region of the 1D ^{1}H NMR spectra of peptides **1**–**8** as an example.

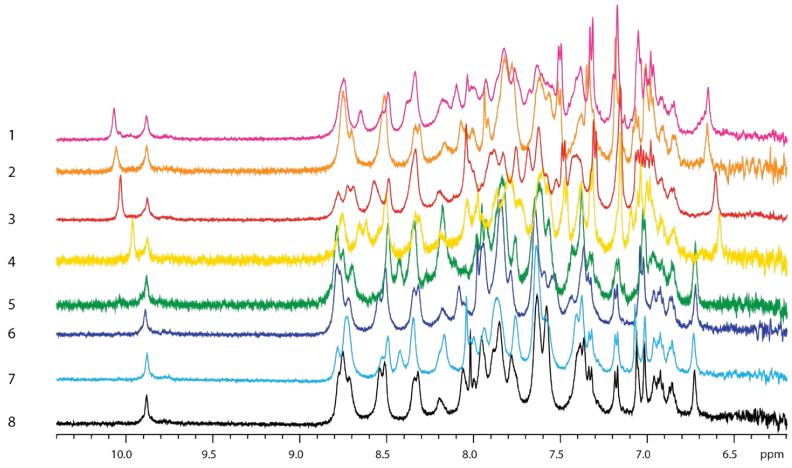

Supplementary Figure 5. Amide region of the 1D ^{1}H NMR spectra for peptides **1**-**8**. Data were collected on a 500 MHz magnet with a sample consisting of 200 μM peptide, 20 mM sodium phosphate (pH 7) with 10% D_2O. Resonances at 9.8-

10.2 ppm represent the indole proton(s) from the two Trp residues in 1-4 (Trp14 and Trp30), or the single Trp residue in 5-8 (Trp 30).

3. Crystallographic Characterization of Peptide 1

Crystal form 1: Peptide **1** was crystallized by vapor diffusion in sitting drops where the well solution contained 50% (v/v) PEG-200 + 0.1M Na/K phosphate, pH 6.2 + 0.2 M NaCl). Each drop contained 0.3 µl well solution + 0.3 µl protein (5-10 mg/mL in water). Crystals were briefly dipped in cryoprotectant (25 % (v/v) glycerol in well solution), then cryo-cooled by plunging into liquid nitrogen prior to data collection. Data were collected at 100 K with a copper rotating anode X-ray source (Rigaku Micromax-007HF), with Varimax-HR confocal optics, and a Rigaku Raxis4++ image plate detector.

Crystal form 2: Peptide **1** was crystallized by vapor diffusion in hanging drops where the well solution contained 30% (v/v) Jeffamine ED-2001 + 0.1 M HEPES + pH 7.0). Each drop contained 2 µl well solution + 2 µl protein. Crystals were cryo-cooled by plunging into liquid nitrogen prior to data collection. Data were collected at 100 K with a copper rotating anode X-ray source (Rigaku Micromax-007HF), with Varimax-HR confocal optics, and a Rigaku Raxis4++ image plate detector.

Data for **Crystal form 1** was integrated and scaled using HKL-2000.[7] The space group for **Crystal form 1** was determined to be C2 with unit cell parameters 84.8 Å, 38.5 Å, 37.0 Å. The asymmetric unit was predicted to contain three copies of the 33-residue construct based on the predicted solvent content of the crystal (Matthew Coefficient). The structure was determined by molecular replacement with Phaser (CCP4 program suite) using the coordinates of the structure obtained for **Crystal form 2** with all residues truncated to a alanine as the search model. The initial electron density map indicated three copies of the helix assembled in a coiled coil; side-chain density was clearly interpretable. Model building was carried out using COOT.[8] Refinement was performed with Phenix.[9]

Data for **Crystal form 2** was integrated and scaled using HKL-2000.[7] The space group for **Crystal form 2** was determined to be R3 with unit cell parameters 39.4 Å, 39.4 Å, 98.7 Å. The asymmetric unit was predicted to contain 2 copies of the 33-residue construct based on the predicted solvent content of the crystal

(Matthew Coefficient). The structure was determined by molecular replacement with Phaser (CCP4 program suite) using the coordinates of the a coiled-coil trimer structure previously determined.[10] The initial electron density map indicated two helix bundles, each containing three helices; side-chain density was clearly interpretable. Model building was carried out using COOT.[8] Refinement was performed with Phenix.[9] Coordinates were deposited in the Protein Data Bank, with PDB ID 5UXT.

Supplementary Table 7. Crystal structure statistics for **Crystal forms 1 and 2** of peptide **1**

Data collection (Crystal form 1)		**Data collection (Crystal form 2)**	
Space Group	C2	Space Group	R3
Unit cell dimensions (Å)	84.8, 38.5, 37.0	Unit cell dimensions (Å)	39.4, 39.4, 98.7
Resolution (Å)	40-2.20	Resolution (Å)	40-1.80
Total Observations	20,692	Total Observations	39121
Unique observations	6,128	Unique observations	5325
Redundancy	3.9	Redundancy	7.3
Completeness (%)	92 (62.7)	Completeness (%)	99.1 (91.4)
<I/σI>	4 (1.0)	<I/σI>	5(0.5)
Rpim	0.073 (0.265)	Rpim	0.028 (1.919)
Refinement		**Refinement**	
Resolution (Å)	40-2.20	Resolution (Å)	40-1.80
Rcryst[b]	0.194 (0.239)	Rcryst[b]	0.238
Rfree[c]	0.275 (0.337)	Rfree[c]	0.278
<B> (Å^2): all atoms / # atoms	44.6 / 845	<B> (Å^2): all atoms / # atoms	55.0/523
<B> (Å^2): water molecules / #water	46.3 / 57	<B> (Å^2): water molecules / #water	55.3/14
RMSD: bonds (Å) / angles (°)	0.007 / 0.838	RMSD: bonds (Å) / angles (°)	0.007/0.950

4. Justification for using Ser at position 14 instead of Ala as a control for evaluating Trp-based enhancement of the Glu10-Lys18 Interaction

In the main text, we demonstrated that placing Trp at position 14 enhances the strength of a long-range *i* to *i*+8 Glu10-Lys18 salt bridge better than does Ser. We chose Ser as a negative control because of its polar character and small size, and because it occupies this position in the sequence of the original 1CW coiled coil from which our variants were derived. However, we wondered whether the use of Ser as a negative control instead of the more conventional Ala might have artificially inflated the observed impact of Trp on the Glu10-Lys18 interaction. To explore this possibility, we prepared peptides **24**, **24-AAK**, **24-EAA**, and **24-AAA**, derivatives of peptides **5-8** in which Ala occupies position 14 instead of Ser (Supplementary Table 5). Variable temperature CD experiments revealed that peptides **24**, **24-AAK**, **24-EAA**, and **24-AAA** are too stable in 20 mM sodium phosphate buffer (pH 7) to reliably identify a fully unfolded baseline, and therefore we were unable to extract folding free energy values for these peptides under these conditions. However, we were able to fit variable temperature CD data for peptides **24**, **24-AAK**, **24-EAA**, and **24-AAA** in 20 mM sodium phosphate (pH 7) + 1 M urea; we have folding free energy data for peptides **1-8** under identical conditions (Supplementary Table 12). We observed that impact of Trp relative to Ala on the Glu10-Lys18 interaction is substantially larger than the impact of Trp relative to Ser (Supplementary Table 13). These results indicate that using Ser as a negative control leads to a smaller, more conservative estimate for Trp-based enhancement of the Glu10-Lys18 interaction than when Ala is used as negative control, suggesting that our concerns were unfounded.

Supplementary Table 8. Sequences and folding free energies of GCN4-p1 variants **20**, **21**, **22** and their derivatives.[a]

Peptide	Sequence	ΔG_f (kcal/mol) in 1M Urea
1	Ac–EVEALEKKV**E**ALE**W**KVQ**K**LEKKVEALEHGWDGR–$CONH_2$	-16.23 ± 0.05
2	Ac–EVEALEKKV**AA**LE**W**KVQ**K**LEKKVEALEHGWDGR–$CONH_2$	-15.73 ± 0.04
3	Ac–EVEALEKKV**E**ALE**W**KVQ**A**LEKKVEALEHGWDGR–$CONH_2$	-14.04 ± 0.03
4	Ac–EVEALEKKV**AA**LE**W**KVQ**A**LEKKVEALEHGWDGR–$CONH_2$	-15.78 ± 0.05
5	Ac–EVEALEKKV**E**ALE**S**KVQ**K**LEKKVEALEHGWDGR–$CONH_2$	-13.42 ± 0.02
6	Ac–EVEALEKKV**AA**LE**S**KVQ**K**LEKKVEALEHGWDGR–$CONH_2$	-14.74 ± 0.02
7	Ac–EVEALEKKV**E**ALE**S**KVQ**A**LEKKVEALEHGWDGR–$CONH_2$	-14.18 ± 0.02
8	Ac–EVEALEKKV**AA**LE**S**KVQ**A**LEKKVEALEHGWDGR–$CONH_2$	-15.30 ± 0.04
24	Ac–EVEALEKKV**E**ALE**A**KVQ**K**LEKKVEALEHGWDGR–$CONH_2$	-14.78 ± 0.02
24-AAK	Ac–EVEALEKKV**AA**LE**A**KVQ**K**LEKKVEALEHGWDGR–$CONH_2$	-16.66 ± 0.07
24-EAA	Ac–EVEALEKKV**E**ALE**A**KVQ**A**LEKKVEALEHGWDGR–$CONH_2$	-16.31 ± 0.06
24-AAA	Ac–EVEALEKKV**AA**LE**A**KVQ**A**LEKKVEALEHGWDGR–$CONH_2$	-17.32 ± 0.09

[a]Data are given ± standard error at 30 μM protein concentration in 20 mM sodium phosphate buffer (pH 7) + 1 M urea at 343.15 K.

Supplementary Table 9. Impact of Trp14 relative to Ser14 or Ala14 on the long-range interaction between Glu10 and Lys18 in the homotrimeric 1CW coiled coil.[a]

	$\Delta\Delta\Delta G_f$ (kcal/mol)
Impact of Trp vs. Ser on the Glu10-Lys18 Interaction	-2.45 ± 0.10
Impact of Trp vs. Ala on the Glu10-Lys18 Interaction	-3.12 ± 0.15

[a]Data are given ± standard error at 30 μM protein concentration in 20 mM sodium phosphate buffer (pH 7) + 1M urea at 343.15 K. Triple mutant cycle analysis performed for peptides **1**–**4** in comparison to Ser-containing peptides **5**–**8**, vs. Ala-containing peptides **24-AAK**, **24-EAA**, **24-AAA**.

5. Enhancing a long-range salt bridge in an additional α-helical model system

We wondered whether the ability of an i+4 non-polar amino acid to enhance the stability of a long-range salt-bridge between an *i*-position Glu and an *i*+8 position Lys might also apply in other α-helices in addition to the homotrimeric model system described in the main text. We decided explore this possibility in the context of the homodimeric α-helical coiled coil GCN4-p1 (sequence shown in Supplementary Table 8). In the native GCN4-p1 sequence, Lys18 already occupies the *i*+8-position relative to Glu10, with Ser14 at *i*+4; all three of these residues lie along the solvent-exposed surface of the coiled-coil homodimer, providing an ideal context for assessing the impact of a non-polar residue at position 14 on the long-range interaction between Glu10 and Lys18. However, we worried that Glu11 (adjacent to Glu10) might interfere with our ability to characterize the Glu10-Lys18 interaction. Consequently, in preparing peptide **20** (in which Glu, Phe, and Lys occupy positions 10, 14, and 18, respectively), we also mutated Glu11 to Ala (see Supplementary Table 8). Circular dichroism (CD) experiments and size-exclusion chromatography experiments indicate that these mutations do not substantially disrupt the homodimeric α-helical coiled-coil quaternary structure of **20** relative to GCN4-p1.

As we did in the main text, we assessed the impact of Phe14 on the Glu10-Lys18 interaction by replacing Glu10 with Ala; Phe14 with Ser; and/or Lys18 with Ala, in all possible combinations. The sequences of **20** and its seven sequence variants appear in Supplementary Table 8, along with folding free energies (from variable temperature CD experiments). Comparing the folding free energies of **20-ESK**, **20-ASK**, **20-ESA**, and **20-ASA** reveals that Glu10 and Lys18 do not interact favorably ($\Delta\Delta\Delta G_f = 0.59 \pm 0.09$ kcal/mol) in the presence of Ser14. In contrast with our previous observations described in the main text, placing Phe at position 14 in the GCN4 system does not substantially change the already unfavorable interaction between Glu10 and Lys18 ($\Delta\Delta\Delta G_f = 0.65 \pm 0.07$ kcal/mol), suggesting that Phe14 does not enhance a long-range salt-bridge between Glu10 and Lys18 (Supplementary Table 9)

It is possible that subtle geometric differences between the homodimeric 1CW system and the homotrimeric system described in the main text might move Glu10 far enough away from Phe14 and Lys18 as to prevent any

Phe-based enhancement in a long-range Glu10-Lys18 interaction. Position 11 occupies the same solvent-exposed face of the helix as Glu10, Phe14, and Lys18 but should be closer to Phe14 and Lys18 than position 10. We wondered whether placing Glu at position 11 instead of position 10, might facilitate a favorable long-range *i* to *i*+7 salt bridge between Glu11 and Lys18 in the presence of Phe14. To test this hypothesis, we prepared peptide **21**, in which Glu, Phe, and Lys occupy positions 11, 14, and 18, respectively, with Ala at position 10 instead of Glu (again, to avoid interference of Glu10 with any possible interaction among Glu11, Phe14, and Lys18). We also prepared variants of **21** in which we replaced Glu11 with Ala; Phe14 with Ser; and/or Lys18 with Ala, in all possible combinations (names and sequences of these variants are shown in Supplementary Table 8; some of these combinations were already accounted for above in peptides **20-AFK**, **20-AFA**, **20 ASK**, and **20-ASA**). Comparing the folding free energies of peptides **21-ESK**, **21-ESA**, **20-ASK**, and **20-ASA** reveals that Glu11 and Lys18 do not interact favorably in the presence of Ser14 ($\Delta\Delta\Delta G_f$ = 1.20 ± 0.07 kcal/mol). However, in the presence of Phe14 (compare peptides **21-EFK**, **21-EFA**, **21-AFK**, and **21-AFA**), the Glu11-Lys18 interaction is substantially favorable ($\Delta\Delta\Delta G_f$ = -0.38 ± 0.07 kcal/mol), a dramatic Phe-based shift of -1.58 ± 0.10 kcal/mol (Supplementary Table 9).

We wondered whether cyclohexylalanine (Cha) would as able to enhance the Glu11-Lys18 interaction in GCN4 as was Phe. To explore this possibility, we prepared peptide **22**, in which Glu, Cha, and Lys occupy positions 11, 14, and 18, respectively. We also prepared variants **22-AXK**, **22-EXA**, and **22-ESA**, in which Glu11 and/or Lys18 have been replaced with Ala in all possible combinations (Supplementary Table 1). Comparing the folding free energies of these variants with those of Ser-containing peptides **21-ESK**, **21-ESA**, **20-ASK**, and **20-ASA** reveals that cyclohexylalanine has as nearly as favorable an impact on the Glu11-Lys18 interaction ($\Delta\Delta\Delta\Delta G_f$ = -1.30 ± 0.09 kcal/mol) as phenylalanine (Supplementary Table 9).

Supplementary Table 10. Sequences and folding free energies of GCN4-p1 variants **20**, **21**, **22** and their derivatives.[a]

Peptide	Sequence	ΔG_f (kcal/mol)
GCN4-p1	Ac–RMKQLEDKVEELESKNYKLENEVARLKKLVGER–$CONH_2$	
20	Ac–RMKQLEDRV**E**ALE**F**KNY**K**LENEVARLKKLVGER–$CONH_2$	-5.57 ± 0.06
20-AFK	Ac–RMKQLEDRV**AA**LE**F**KNY**K**LENEVARLKKLVGER–$CONH_2$	-7.98 ± 0.04
20-EFA	Ac–RMKQLEDRV**E**ALE**F**KNY**A**LENEVARLKKLVGER–$CONH_2$	-6.38 ± 0.04
20-AFA	Ac–RMKQLEDRV**AA**LE**F**KNY**A**LENEVARLKKLVGER–$CONH_2$	-8.14 ± 0.03
20-ESK	Ac–RMKQLEDRV**E**ALE**S**KNY**K**LENEVARLKKLVGER–$CONH_2$	-4.92 ± 0.08
20-ASK	Ac–RMKQLEDRV**AA**LE**S**KNY**K**LENEVARLKKLVGER–$CONH_2$	-7.43 ± 0.02
20-ESA	Ac–RMKQLEDRV**E**ALE**S**KNY**A**LENEVARLKKLVGER–$CONH_2$	-5.85 ± 0.02
20-ASA	Ac–RMKQLEDRV**AA**LE**S**KNY**A**LENEVARLKKLVGER–$CONH_2$	-7.81 ± 0.04
21	Ac–RMKQLEDRVA**E**LE**F**KNY**K**LENEVARLKKLVGER–$CONH_2$	-7.97 ± 0.04
21-EFA	Ac–RMKQLEDRVA**E**LE**F**KNY**A**LENEVARLKKLVGER–$CONH_2$	-7.74 ± 0.02
21-ESK	Ac–RMKQLEDRVA**E**LE**S**KNY**K**LENEVARLKKLVGER–$CONH_2$	-5.60 ± 0.05
21-ESA	Ac–RMKQLEDRVA**E**LE**S**KNY**A**LENEVARLKKLVGER–$CONH_2$	-7.14 ± 0.02
22	Ac–RMKQLEDRVA**E**LE**X**KNY**K**LENEVARLKKLVGER–$CONH_2$	-7.97 ± 0.03
22-AXK	Ac–RMKQLEDRVA**A**LE**X**KNY**K**LENEVARLKKLVGER–$CONH_2$	-8.80 ± 0.02
22-EXA	Ac–RMKQLEDRVA**E**LE**X**KNY**A**LENEVARLKKLVGER–$CONH_2$	-8.19 ± 0.03
22-AXA	Ac–RMKQLEDRVA**A**LE**X**KNY**A**LENEVARLKKLVGER–$CONH_2$	-9.10 ± 0.04

[a]Data are given ± standard error at 30 μM protein concentration in 20 mM sodium phosphate buffer (pH 7) at 333.15 K. **X** = cyclohexylalanine.

Supplementary Table 11. Impact of Phe14 or Cha14 vs. Ser14 on the long-range interaction between Glu and Lys in the homodimeric GCN4-p1 coiled coil.[a]

Peptide	Sequence	Salt-bridge with Ser14 $\Delta\Delta\Delta G_f$ (kcal/mol)	Salt-bridge with Phe14 or Cha14 $\Delta\Delta G_f$ (kcal/mol)	Influence of Phe14 or Cha14 $\Delta\Delta\Delta\Delta G_f$ (kcal/mol)
20	Ac–RMKQLEDRV**E**ALE**F**KNY**K**LENEVARLKKLVGER–$CONH_2$	0.59 ± 0.09	0.65 ± 0.07	0.06 ± 0.12
21	Ac–RMKQLEDRVA**E**LE**F**KNY**K**LENEVARLKKLVGER–$CONH_2$	1.20 ± 0.07	-0.38 ± 0.07	-1.58 ± 0.10
22	Ac–RMKQLEDRVA**E**LE**X**KNY**K**LENEVARLKKLVGER–$CONH_2$	1.20 ± 0.07	-0.09 ± 0.06	-1.30 ± 0.09

[a]Data are given ± standard error at 30 μM protein concentration in 20 mM sodium phosphate buffer (pH 7) at 333.15 K. **X** = cyclohexylalanine. Triple mutant cycle analysis performed for **20**, **21**, and **22** in comparison to **20-AFK**, **20-EFA**, **20-AFA**, **20-ESK**, **20-ASK**, **20-ESA**, **20-ASA**, **21-EFA**, **21-ESK**, **21-ESA**, **22-AXK**, **22-EXA**, **22-AXA**.

6. Impact of Salt on Phe-based enhancement of the Glu10-Lys18 Interaction

We wondered whether the ability of Phe to enhance the long-range Glu10-Lys18 interaction depends on the concentration of salt in the buffer. To explore this possibility, we performed triplicate variable temperature CD experiments on peptides 5–8, 16, 16-AFK, 16-EFA, and 16-AFA in 20 mM sodium phosphate (pH 7) and 0.25 M NaCl. The results of this analysis are shown in Supplementary Tables 14 and 15. The impact of Phe on the Glu10-Lys18 interaction gets stronger in the presence of 0.25 M NaCl, indicating that it is resistant to screening by salt.

Supplementary Table 12. Sequences, expected and observed exact masses, and folding free energies peptides **5**–**8**, **16, 16-AFK**, **16-EFA**, and **16-AFA**.[a]

Peptide	Sequence	ΔG_f (kcal/mol)
5	Ac–EVEALEKKV**E**ALE**S**KVQ**K**LEKKVEALEHGWDGR–$CONH_2$	-14.60 ± 0.02
6	Ac–EVEALEKKV**AA**LE**S**KVQ**K**LEKKVEALEHGWDGR–$CONH_2$	-16.12 ± 0.03
7	Ac–EVEALEKKV**E**ALE**S**KVQ**A**LEKKVEALEHGWDGR–$CONH_2$	-15.77 ± 0.03
8	Ac–EVEALEKKV**AA**LE**S**KVQ**A**LEKKVEALEHGWDGR–$CONH_2$	-17.08 ± 0.05
16	Ac–EVEALEKKV**E**ALE**F**KVQ**K**LEKKVEALEHGWDGR–$CONH_2$	-15.37 ± 0.04
16-AFK	Ac–EVEALEKKV**A**ALE**F**KVQ**K**LEKKVEALEHGWDGR–$CONH_2$	-15.91 ± 0.05
16-EFA	Ac–EVEALEKKV**E**ALE**F**KVQ**A**LEKKVEALEHGWDGR–$CONH_2$	-15.55 ± 0.06
16-AFA	Ac–EVEALEKKV**A**ALE**F**KVQ**A**LEKKVEALEHGWDGR–$CONH_2$	-17.87 ± 0.05

[a]Data are given ± standard error at 30 μM protein concentration in 20 mM sodium phosphate buffer (pH 7) + 0.25 M NaCl at 343.15 K.

Supplementary Table 13. Impact of Phe14 on the long-range interaction between Glu10 and Lys18 in the homotrimeric 1CW coiled coil in 20 mM sodium phosphate (pH 7), with or without 0.25 M NaCl.[a]

	$\Delta\Delta\Delta G_f$ (kcal/mol)
Phe-based stabilization in 20 mM sodium phosphate (pH 7)	-1.25 ± 0.09
Phe-based stabilization in 20 mM sodium phosphate (pH 7) + 0.25 M NaCl	-2.00 ± 0.12

[a]Data are given ± standard error at 30 μM protein concentration in 20 mM sodium phosphate buffer (pH 7) + 0.25 M NaCl at 343.15 K.

7. Phe-based enhancement of the Glu10-Arg18 interaction in the 1CW homotrimeric coiled coil

We wondered whether Phe14 might also be able to enhance a long-range interaction between Glu10 and Arg18 (rather than Lys18) in the context of the 1CW coiled-coil homodimer. To explore this possibility, we prepared peptide **23**, a derivative of main text peptide **16**, in which Glu, Phe, and Arg occupy positiosn 10, 14, and 18, respectively, along with variants **23-AFR**, **23-ESR**, and **23-ASR**. The sequences and folding free energies of these peptides appear in Supplementary Table 10, along with those of peptides **5-8** and **16**, **16-AFK**, **16-EFA**, and **16-AFA**, for comparison. We used triple mutant cycle analysis to compare the impact of Phe on the Glu10-Lys18 interaction vs. the Glu10-Arg18 interaction. The results of this analysis appear in Supplementary Table 11. We find that Phe enhances the Glu10-Arg18 interaction by a slightly larger amount ($\Delta\Delta\Delta\Delta G_f$ = -1.52 ± 0.09 kcal/mol) than it does the Glu10-Lys18 interaction ($\Delta\Delta\Delta\Delta G_f$ = -1.25 ± 0.09 kcal/mol), suggesting that Lys and Arg are similarly amenable to Phe-based enhancement of a long-range salt bridge with Glu10.

Supplementary Table 14. Sequences and folding free energies of GCN4-p1 variants **5-8**, **16**, **16-AFK**, **16-EFA**, **16-AFA**, **20-AFR**, **20-ESR**, and **23-ASR** and their derivatives.[a]

Peptide	Sequence	ΔG_f (kcal/mol)
5	Ac–EVEALEKKV**E**ALE**S**KVQ**K**LEKKVEALEHGWDGR–$CONH_2$	-14.09 ± 0.02
6	Ac–EVEALEKKV**AA**LE**S**KVQ**K**LEKKVEALEHGWDGR–$CONH_2$	-15.87 ± 0.03
7	Ac–EVEALEKKV**E**ALE**S**KVQ**A**LEKKVEALEHGWDGR–$CONH_2$	-15.48 ± 0.02
8	Ac–EVEALEKKV**AA**LE**S**KVQ**A**LEKKVEALEHGWDGR–$CONH_2$	-16.39 ± 0.04
16	Ac–EVEALEKKV**E**ALE**F**KVQ**K**LEKKVEALEHGWDGR–$CONH_2$	-14.66 ± 0.02
16-AFK	Ac–EVEALEKKV**A**ALE**F**KVQ**K**LEKKVEALEHGWDGR–$CONH_2$	-16.18 ± 0.03
16-EFA	Ac–EVEALEKKV**E**ALE**F**KVQ**A**LEKKVEALEHGWDGR–$CONH_2$	-15.05 ± 0.03
16-AFA	Ac–EVEALEKKV**A**ALE**F**KVQ**A**LEKKVEALEHGWDGR–$CONH_2$	-16.95 ± 0.04
23	Ac–EVEALEKKV**E**ALE**F**KVQ**R**LEKKVEALEHGWDGR–$CONH_2$	-15.65 ± 0.02
23-AFR	Ac–EVEALEKKV**A**ALE**F**KVQ**R**LEKKVEALEHGWDGR–$CONH_2$	-16.84 ± 0.03
23-ESR	Ac–EVEALEKKV**E**ALE**S**KVQ**R**LEKKVEALEHGWDGR–$CONH_2$	-14.59 ± 0.02
23-ASR	Ac–EVEALEKKV**A**ALE**S**KVQ**R**LEKKVEALEHGWDGR–$CONH_2$	-16.30 ± 0.03

[a]Data are given ± standard error at 30 μM protein concentration in 20 mM sodium phosphate buffer (pH 7) at 343.15 K.

Supplementary Table 15. Impact of Phe14 vs. Ser14 on the long-range interaction between Glu10 and Lys18 or Arg18 in the homotrimeric 1CW coiled coil.[a]

Peptide	Influence of Phe14 vs. Ser14 $\Delta\Delta\Delta\Delta G_f$ (kcal/mol)
Glu10-Lys18	-1.25 ± 0.09
Glu10-Arg18	-1.52 ± 0.09

[a]Data are given ± standard error at 30 μM protein concentration in 20 mM sodium phosphate buffer (pH 7) at 343.15 K. Triple mutant cycle analysis performed for **16** and **23** in comparison to peptides **5**–**8**, **16-AFK**, **16-EFA**, **16-AFA**, **23-AFR**, **23-ESR**, **23-ESA**.

References

1. Pandey, B.K. et al. Impact of Site-Specific PEGylation on the Conformational Stability and Folding Rate of the Pin WW Domain Depends Strongly on PEG Oligomer Length. *Bioconjugate Chem.* **24**, 796-802 (2013).
2. Ciani, B. et al. Molecular basis of coiled-coil oligomerization-state specificity. *Proceedings of the National Academy of Sciences of the United States of America* **107**, 19850-19855 (2010).
3. Spector, S., Young, P. & Raleigh, D.P. Nativelike structure and stability in a truncation mutant of a protein minidomain: The peripheral subunit-binding domain. *Biochemistry* **38**, 4128-4136 (1999).
4. Ogihara, N., Weiss, M., Degrado, W. & Eisenberg, D. The crystal structure of the designed trimeric coiled coil coil-VaLd: implications for engineering crystals and supramolecular assemblies. *Protein Sci.* **6**, 80–88 (1997).
5. Woolfson, D.N. & Alber, T. Predicting Oligomerization States of Coiled Coils. *Protein Sci.* **4**, 1596–1607 (1995).
6. Edelhoch, H. Spectroscopic Determination of Tryptophan and Tyrosine in Proteins*. *Biochemistry* **6**, 1948-1954 (1967).
7. Otwinowski, Z. & Minor, W. Processing of X-ray diffraction data collected in oscillation mode. *Macromolecular Crystallography, Pt A* **276**, 307-326 (1997).
8. Emsley, P., Lohkamp, B., Scott, W.G. & Cowtan, K. Features and development of Coot. *Acta Crystallographica Section D-Biological Crystallography* **66**, 486-501 (2010).
9. Adams, P.D. et al. PHENIX: a comprehensive Python-based system for macromolecular structure solution. *Acta Crystallographica Section D-Biological Crystallography* **66**, 213-221 (2010).
10. Ogihara, N.L., Weiss, M.S., Degrado, W.F. & Eisenberg, D. The crystal structure of the designed trimeric coiled coil coil-V(a)L(d): Implications for engineering crystals and supramolecular assemblies. *Protein Science* **6**, 80-88 (1997).